

Electromagnetically induced transparency for x rays

Christian Buth, Robin Santra, and Linda Young
Argonne National Laboratory, Argonne, Illinois 60439, USA
(Dated: 10 May 2007)

Electromagnetically induced transparency (EIT) is predicted for x rays in laser-dressed neon gas. The x-ray photoabsorption cross section and polarizability near the Ne *K* edge are calculated using an *ab initio* theory suitable for optical strong-field problems. The laser wavelength is tuned close to the transition between $1s^{-1}3s$ and $1s^{-1}3p$ (~ 800 nm). The minimum laser intensity required to observe EIT is of the order of 10^{12} W/cm². The *ab initio* results are discussed in terms of an exactly solvable three-level model. This work opens new opportunities for research with ultrafast x-ray sources.

PACS numbers: 32.30.Rj, 32.80.Fb, 32.80.Rm, 42.50.Hz

In a Λ -type medium characterized by atomic levels a , b , and c with energies $E_a > E_b > E_c$, resonant absorption on the $c \rightarrow a$ transition can be strongly suppressed by simultaneously irradiating the medium with an intense laser that couples the levels a and b . This phenomenon is known as electromagnetically induced transparency (EIT) [1, 2, 3]. EIT enables one to control the absorption and dispersion of a gaseous medium. It has become a versatile tool for creating media with exceptional optical properties [4, 5, 6, 7]. EIT forms the basis of a recent proposal for a high-accuracy optical clock [8].

In this Letter, we study EIT for x rays. Specifically, we consider the near-*K*-edge structure of neon gas in the presence of a linearly polarized 800-nm laser with an intensity of 10^{13} W/cm². The decay widths of excited states involved in EIT in the optical regime typically do not exceed $\sim 10^{-4}$ eV (see, e.g., Ref. [2]) and are often much smaller. In contrast, the decay width of core-excited neon, $\Gamma_{1s} = 0.27$ eV [9], is larger by a factor of ~ 2000 . Therefore, as we will show below, the intensity of the coupling laser must be extraordinarily high. This represents the first case of EIT where the laser causes strong-field ionization of the two upper levels.

Because of their high binding energy, the core and valence electrons of Ne remain essentially unperturbed at 10^{13} W/cm². (Multiphoton ionization of Ne in its ground state is negligible.) However, laser dressing of the core-excited states introduces strong-field physics: For the laser parameters employed here, the ponderomotive potential [10] is $U_p = 0.60$ eV, and the energy needed to ionize, for instance, the $3p$ electron in the $1s^{-1}3p$ state is $I_{1s^{-1}3p} = 2.85$ eV ($1s^{-1}3p$ denotes the state produced by exciting a $1s$ electron to the $3p$ Rydberg orbital). Hence, the Keldysh parameter [11] is $\gamma = \sqrt{I_{1s^{-1}3p}/(2U_p)} = 1.5$. For $\gamma \ll 1$, the atom-field interaction can be described in the adiabatic tunneling picture; the perturbative multiphoton regime is indicated by $\gamma \gg 1$. In our case, where $\gamma \approx 1$, the nonadiabatic strong-field regime persists; neither perturbation theory nor a tunneling description is adequate. It should also be noted that the transition energy between, e.g., the states

$1s^{-1}3s$ and $1s^{-1}3p$ is 1.69 eV, which is, within the decay width of the core-excited states, in one-photon resonance with the 1.55-eV laser.

For this intermediate intensity regime, we have developed the *ab initio* theory described in Ref. [12]. Briefly, the electronic structure of the atom is described in the Hartree-Fock-Slater approximation; nonrelativistic quantum electrodynamics is used to treat the interaction of the atom with the two-color radiation field consisting of the dressing laser and the x rays. Our calculations were carried out with the DREYD program [13]. We used the computational parameters from Ref. [12], with the exception that for the atomic basis, we included angular momentum quantum numbers $l = 0, \dots, 9$, and for the laser-photon basis, we included the simultaneous emission and absorption of up to 20 photons. The non-Hermitian Hamiltonian matrix (dimension 41000) was diagonalized using a Lanczos algorithm for complex-symmetric matrices [14]. All results are converged with respect to the electronic and photonic basis sets and the number of Lanczos iterations.

The calculated x-ray photoabsorption cross section of a neon atom is displayed in Fig. 1 for three cases. (The x rays are assumed to be linearly polarized.) First, there is the cross section without laser dressing, $\sigma_{1s,n.l.}(\omega_X)$. Second is shown the cross section for parallel laser and x-ray polarization vectors, $\sigma_{1s}^{\parallel}(\omega_X) \equiv \sigma_{1s}(\omega_X, 0^\circ)$. In the third case, the polarization vectors are perpendicular, $\sigma_{1s}^{\perp}(\omega_X) \equiv \sigma_{1s}(\omega_X, 90^\circ)$. Our result for $\sigma_{1s,n.l.}(\omega_X)$ is in good agreement with experimental and theoretical data [15, 16]. The prominent absorption feature at 867.4 eV arises due to excitation into the $1s^{-1}3p$ state. The weaker peaks are associated with $1s \rightarrow np$ transitions with $n \geq 4$. The *K* edge lies at 870.2 eV [9].

Exposing neon to intense laser light shifts and mixes the atomic energy levels. This leads to the pronounced differences between the laser-on and laser-off cases in Fig. 1. Nevertheless, in spite of the rather high laser intensity, there is still substantial structure in both $\sigma_{1s}^{\parallel}(\omega_X)$ and $\sigma_{1s}^{\perp}(\omega_X)$. The absorption peaks are broader by about a factor of two in comparison to the laser-free case. This

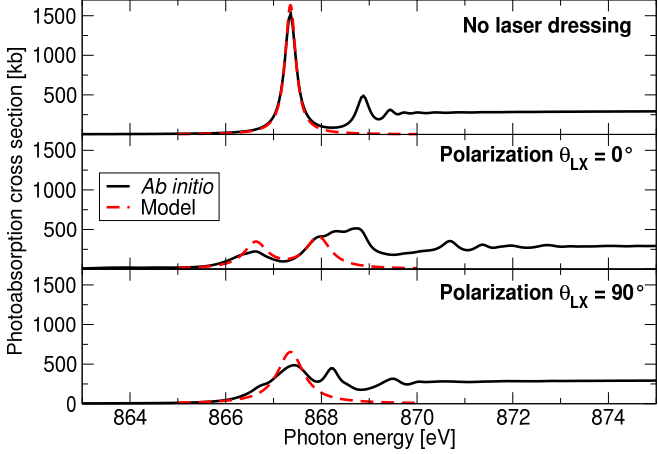


FIG. 1: X-ray photoabsorption cross section of neon near the K edge with laser dressing [$\sigma_{1s}(\omega_X, \theta_{LX})$] and without it [$\sigma_{1s,n.l.}(\omega_X)$]. Results from *ab initio* calculations and a three-level model are shown. Here, θ_{LX} is the angle between the polarization vectors of the laser and the x rays. The laser operates at a wavelength of 800 nm and an intensity of 10^{13} W/cm^2 .

is because the laser ionizes the Rydberg electron at a rate that is comparable to the Auger decay rate of the K -shell hole. Therefore, in the presence of the laser, one may expect an enhanced production of Ne^{2+} in the pre- K -edge region. The laser deforms the orbitals cylindrically along the laser polarization axis. Thus, anisotropy arises with respect to the angle θ_{LX} between x-ray and laser polarization vectors. This is the origin of the differences between $\sigma_{1s}^{\parallel}(\omega_X)$ and $\sigma_{1s}^{\perp}(\omega_X)$ [12]. The most eye-catching

impact of the laser dressing can be seen in the vicinity of the $1s \rightarrow 3p$ resonance, which is highly suppressed for $\theta_{LX} = 0^\circ$. As will be explained in the following paragraphs, this suppression of the $1s \rightarrow 3p$ resonance is a manifestation of EIT. The suppression for $\theta_{LX} = 90^\circ$ is a consequence of laser-induced line broadening. We would like to point out that, at least in the case of $\sigma_{1s}^{\parallel}(\omega_X)$, weak structures, not present in $\sigma_{1s,n.l.}(\omega_X)$, emerge above the K edge of the laser-free atom. These are produced by multiphoton processes involving the photoelectron. This is similar to above-threshold ionization [17].

In order to understand the reason for the laser-induced suppression of the $1s \rightarrow 3p$ transition, we reduce the *ab initio* theory of Ref. [12] to a Λ -type model. To this end, we identify the levels a , b , and c mentioned earlier with the states $1s^{-1} 3p$, $1s^{-1} 3s$, and the atomic ground state, respectively. Levels a and b are decaying states, due to both Auger decay and laser ionization, with widths Γ_a and Γ_b . The energy spacing between a and b is symbolized by ω_{ab} ; similarly, ω_{ac} denotes the spacing between a and c . The Hamiltonian \hat{H} is the sum of the atomic Hamiltonian \hat{H}_{AT} , the free electromagnetic field \hat{H}_{EM} , the laser-electron interaction \hat{H}_{L} , and the x-ray-electron interaction \hat{H}_{X} . The Hamiltonian \hat{H} is represented in the direct product basis $\{|c\rangle|N_L\rangle|N_X\rangle, |b\rangle|N_L+1\rangle|N_X-1\rangle, |a\rangle|N_L\rangle|N_X-1\rangle\}$, where $|N_L\rangle$ and $|N_X\rangle$ are Fock states of the laser and x-ray modes, respectively. The strong laser coupling between a and b is treated by diagonalizing \hat{H} in the corresponding subspace. The x-ray coupling of level c to the resulting dressed states is weak and is treated perturbatively. The x-ray photoabsorption cross section obtained in this way is

$$\sigma_{\text{Model}}(\omega_X, \theta_{LX}) = \sigma_0 \text{Im} \left[\cos^2 \theta_{LX} \sum_{s=\pm} \left(\frac{\Omega_{ab}^2/4}{E_s^2 + \Omega_{ab}^2/4} \frac{\gamma_a}{\omega_{ac} - i\gamma_a + E_s - \omega_X} \right) + \sin^2 \theta_{LX} \frac{\gamma_a}{\omega_{ac} - i\gamma_a - \omega_X} \right]. \quad (1)$$

Here, Ω_{ab} is the Rabi frequency [18] associated with levels a and b , $E_{\pm} \equiv -\frac{1}{2}[\omega_{ab} - \omega_L - i(\gamma_a - \gamma_b)] \pm \frac{1}{2}\sqrt{(\omega_{ab} - \omega_L - i(\gamma_a - \gamma_b))^2 + \Omega_{ab}^2}$ is the level shift of the two laser-dressed states, $\gamma_a = \Gamma_a/2$, $\gamma_b = \Gamma_b/2$, and ω_L is the laser photon energy. The parameter σ_0 is the cross section obtained on resonance ($\omega_X = \omega_{ac}$) without laser ($\Omega_{ab} \rightarrow 0$). Let the laser polarization axis coincide with the z axis. Then, at $\theta_{LX} = 90^\circ$, the absorption

cross section is given by a simple Lorentzian [cf. Eq. (1)] because only $1s^{-1} 3p_x$ or $1s^{-1} 3p_y$ can be excited by the x rays. Dipole selection rules dictate that the laser can couple only $1s^{-1} 3p_z$ to $1s^{-1} 3s$. The two dressed states that appear as a consequence of the laser-mediated coupling can be probed by the x rays at $\theta_{LX} = 0^\circ$. Using $\Delta_{LX} \equiv (\omega_{ac} - \omega_X) - (\omega_{ab} - \omega_L)$, we find from Eq. (1) for $\theta_{LX} = 0^\circ$

$$\sigma_{\text{Model}}(\omega_X, 0^\circ) = \sigma_0 \frac{\gamma_a^2 \Delta_{LX}^2 + \gamma_a \gamma_b (\Omega_{ab}^2/4 + \gamma_a \gamma_b)}{[\Omega_{ab}^2/4 + \gamma_a \gamma_b - \Delta_{LX} (\omega_{ac} - \omega_X)]^2 + [\gamma_a \Delta_{LX} + \gamma_b (\omega_{ac} - \omega_X)]^2}. \quad (2)$$

This expression is identical to the absorption cross section given in Ref. [2] for EIT in a Λ -type model. Because the lifetime of the laser-dressed core-excited states considered here is only of the order of 1 fs, we neglect other decoherence mechanisms such as collisional broadening. If the width γ_b in Eq. (2) were zero ($\gamma_a \neq 0$, $\Omega_{ab} \neq 0$), then the absorption cross section would vanish completely provided the resonance condition $\Delta_{\text{LX}} = 0$ is satisfied. (See Ref. [8] for an example.) For finite γ_b , there is in general a suppression of absorption on resonance. In view of Eq. (1), this suppression of absorption characteristic of EIT is due to the destructive interference of the excitation pathways from the atomic ground state to the two laser-dressed core-excited states.

The x-ray photoabsorption cross section of the model, Eq. (1), is displayed in Fig. 1 together with the *ab initio* data. The agreement for $\sigma_{1s,\text{n.l.}}(\omega_X)$ is excellent, illustrating that the absorption line at 867.4 eV is nearly exclusively caused by the $1s \rightarrow 3p$ transition. As far as level energies and transition dipole matrix elements are concerned, the model and *ab initio* calculations share the same input data. However, in the *ab initio* treatment, the laser is allowed to couple $1s^{-1} 3s$ and $1s^{-1} 3p$ to states outside the three-level subspace. This coupling leads to both additional AC Stark shifts [18] and ionization broadening of levels a and b . We account for the ionization broadening in the presence of the laser by assuming effective linewidths $\Gamma_a = 0.675$ eV and $\Gamma_b = 0.54$ eV. These parameters give reasonable agreement with the *ab initio* results for $\sigma_{1s}^{\parallel}(\omega_X)$ and $\sigma_{1s}^{\perp}(\omega_X)$ in the vicinity of the $1s \rightarrow 3p$ resonance. The AC Stark shifts due to states outside the three-level subspace are apparently small and are neglected in the model. The model reproduces the double-hump structure in $\sigma_{1s}^{\parallel}(\omega_X)$ and, in particular, the suppression of the $1s \rightarrow 3p$ resonance. This agreement leads us to conclude that the dominant physics here is EIT.

Because of the rather large decay widths Γ_a and Γ_b , the EIT structure seen in $\sigma_{1s}^{\parallel}(\omega_X)$ is relatively insensitive to changes $\Delta\omega_L$ of the laser photon energy. We find that EIT persists for $\Delta\omega_L/\omega_L \approx 30\%$. In accordance with the approximate EIT resonance condition $\Delta_{\text{LX}} = 0$, the x-ray absorption minimum is shifted by $\sim \Delta\omega_L$. A simple criterion for the laser intensity required to observe a significant EIT effect can be found as follows. The laser photon energy ω_L is chosen to be in exact resonance with levels a and b . EIT appears when the real parts of the two pole positions in Eq. (1) [$\theta_{\text{LX}} = 0^\circ$] are separated by more than the Auger width Γ_{1s} (laser broadening of the lines is neglected here). The required laser intensity thus follows from the relation $|\Omega_{ab}| > \Gamma_{1s}$; we calculate $I_L > 4.3 \times 10^{11} \text{ W/cm}^2$. This estimate is, in fact, somewhat too optimistic: We varied the intensity in the *ab initio* calculation for an 800-nm dressing laser and found appreciable EIT for $I_L > 10^{12} \text{ W/cm}^2$.

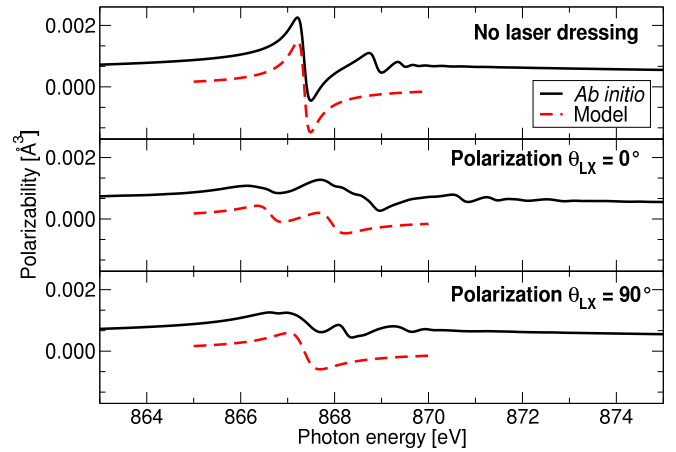


FIG. 2: Dynamic polarizability of atomic neon near the K edge. See the caption of Fig. 1 for details.

The EIT signature is particularly clear for intensities around 10^{13} W/cm^2 , the value used for Fig. 1. Because of the strong perturbation by the laser field, the splitting between the two EIT peaks is only approximately given by the Rabi frequency $|\Omega_{ab}|$.

For a complete characterization of the x-ray properties of laser-dressed atoms, we need—in addition to the absorption cross section—the dynamic (i.e., photon-energy-dependent) polarizability $\alpha(\omega_X, \theta_{\text{LX}})$. As will be described elsewhere, $\alpha(\omega_X, \theta_{\text{LX}})$ may be calculated using an extension of the formalism of Refs. [12] and [19]. The dynamic polarizability of neon is plotted in Fig. 2 for the three cases considered in Fig. 1. Both *ab initio* and three-level model results are depicted. Apart from a missing background due to states outside the three-level subspace, the model reproduces the structure of $\alpha(\omega_X, \theta_{\text{LX}})$ in the vicinity of the $1s \rightarrow 3p$ resonance. The dynamic polarizability (together with the number density and the number of electrons per atom) determines the index of refraction. As one can see in Fig. 2, the primary impact of laser dressing on $\alpha(\omega_X, \theta_{\text{LX}})$ is the suppression of dispersion near the resonance. This is in contrast to the situation encountered in the optical domain [7]. Using the *ab initio* data shown in Fig. 2, we calculate that in the EIT case ($\theta_{\text{LX}} = 0^\circ$), the x-ray group velocity at the $1s \rightarrow 3p$ resonance is reduced relative to the speed of light by only 3×10^{-6} . (A neon pressure of one atmosphere is assumed.) It therefore seems likely that EIT is most suitable for amplitude modulation, rather than phase modulation, of x rays.

In practice, high intensities are achieved using short-pulse lasers. For instance, if one operates a Ti:Sapphire laser system at a repetition rate of $\sim 1 \text{ kHz}$, the typical pulse energy per shot is $\sim 1 \text{ mJ}$. With a focal width of, say, $50 \mu\text{m}$, the pulse duration required for a peak intensity of 10^{13} W/cm^2 is of the order of 1 ps. In order to

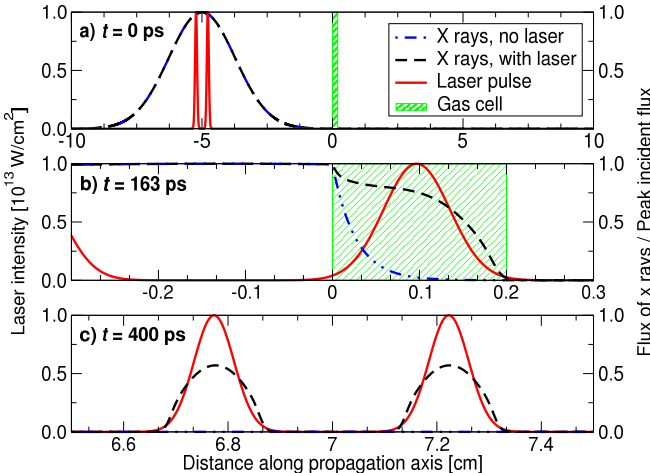


FIG. 3: EIT-based generation of two ultrashort x-ray pulses with well-defined time delay.

maximize the EIT signal, the laser intensity during the exposure of the laser-dressed medium to the x rays must remain high and essentially constant, i.e., the x rays must have a pulse duration of 1 ps or shorter. Such ultrashort x-ray pulses can presently be produced by high-order harmonic generation [20]; laser plasma sources [21]; and the laser slicing method [22, 23]. All three approaches provide a relatively low number of x-ray photons per pulse. The upcoming x-ray free-electron lasers [24, 25, 26] will be high-flux sources of femtosecond x-ray pulses.

A possible experimental scheme for observing the EIT effect discussed here is the following. Consider a 2-mm-long gas cell filled with neon at atmospheric pressure and room temperature, so that the neon number density is $2.4 \times 10^{19} \text{ cm}^{-3}$. In the absence of the laser, the x-ray absorption cross section on the $1s \rightarrow 3p$ resonance is $\sim 1500 \text{ kb}$. Therefore, the linear absorption coefficient is 36 cm^{-1} . Assuming that Beer's law [18] holds, only 0.07% of the x rays are transmitted through the gas cell on resonance. Applying the dressing laser with parallel laser and x-ray polarizations, the x-ray absorption cross section is suppressed by a factor of ~ 13 (see Fig. 1). In this case, the linear absorption coefficient is 2.8 cm^{-1} , and the x-ray transmission on resonance rises to 57%—an increase by a factor of ~ 800 . This effect should be straightforward to measure experimentally.

An exciting prospect is to use this scheme to imprint pulse shapes of the optical dressing laser onto the x rays. To demonstrate the idea, we have numerically propagated a 100-ps x-ray pulse (peak flux 8×10^9 photons/ps/cm 2) together with two 3-ps laser pulses, taking into account the laser intensity dependence of the $1s \rightarrow 3p$ x-ray absorption cross section in the neon gas cell. Three temporal snapshots are shown in Fig. 3. At $t = 0$, the x-ray and laser pulses are still outside the gas cell. After 163 ps, the first of the two laser pulses over-

laps with the x-ray pulse inside the gas cell, thereby substantially enhancing x-ray transmission in comparison to the laser-off case. At $t = 400$ ps, i.e., after propagation through the gas cell, two ultrashort x-ray pulses (~ 5 ps) emerge. The x-ray pulses are somewhat broadened with respect to the laser pulses because of the nonlinear dependence of the x-ray absorption cross section on the laser intensity. The time delay between the two x-ray pulses can be controlled by changing the time delay between the two laser pulses, opening a route to ultrafast all x-ray pump-probe experiments. With an analogous strategy, controlled shaping of short-wavelength pulses might become a reality, similar to the sophisticated techniques already available for optical wavelengths [27]. Estimates show that for the parameters quoted, dispersion effects due to neutral neon atoms dominate over those caused by the rather dilute x-ray-generated plasma. The time delay experienced by both x-ray and laser pulses transmitted through the gas cell is in the sub-fs regime.

We thank T. E. Glover and A. Wagner for fruitful discussions. This work was supported by the Office of Basic Energy Sciences, Office of Science, U.S. Department of Energy, under Contract No. DE-AC02-06CH11357. C.B. was funded by the Alexander von Humboldt Foundation.

- [1] S. E. Harris, J. E. Field, and A. Imamoğlu, Phys. Rev. Lett. **64**, 1107 (1990).
- [2] K.-J. Boller, A. Imamoğlu, and S. E. Harris, Phys. Rev. Lett. **66**, 2593 (1991).
- [3] S. E. Harris, Phys. Today **50**, 36 (1997).
- [4] L. V. Hau *et al.*, Nature **397**, 594 (1999).
- [5] D. F. Phillips *et al.*, Phys. Rev. Lett. **86**, 783 (2001).
- [6] M. Lukin and A. Imamoğlu, Nature **413**, 273 (2001).
- [7] M. Fleischhauer, A. Imamoğlu, and J. P. Marangos, Rev. Mod. Phys. **77**, 633 (2005).
- [8] R. Santra *et al.*, Phys. Rev. Lett. **94**, 173002 (2005).
- [9] V. Schmidt, *Electron spectrometry of atoms using synchrotron radiation* (Cambridge University Press, Cambridge, 1997).
- [10] R. R. Freeman, P. H. Bucksbaum, and T. J. McIlrath, IEEE J. Quantum Electron. **24**, 1461 (1988).
- [11] L. Keldysh, Sov. Phys. JETP **20**, 1307 (1965).
- [12] C. Butth and R. Santra, Phys. Rev. A **75**, 033412 (2007).
- [13] C. Butth *et al.*, FELLA – the free electron laser atomic physics program package, Argonne National Laboratory, Argonne, Illinois, USA (2007), version 1.1.0.
- [14] T. Sommerfeld *et al.*, J. Phys. B **31**, 4107 (1998).
- [15] M. Coreno *et al.*, Phys. Rev. A **59**, 2494 (1999).
- [16] T. W. Gorczyca, Phys. Rev. A **61**, 024702 (2000).
- [17] P. Agostini *et al.*, Phys. Rev. Lett. **42**, 1127 (1979).
- [18] P. Meystre and M. Sargent III, *Elements of quantum optics* (Springer, Berlin, 1991), 2nd ed.
- [19] C. Butth, R. Santra, and L. S. Cederbaum, Phys. Rev. A **69**, 032505 (2004).
- [20] C. Spielmann *et al.*, Science **278**, 661 (1997).
- [21] Y. Jiang, T. Lee, and C. Rose-Petru, J. Opt. Soc. Am.

B **20**, 229 (2003).

[22] R. W. Schoenlein *et al.*, Science **287**, 2237 (2000).

[23] S. Khan *et al.*, Phys. Rev. Lett. **97**, 074801 (2006).

[24] J. Arthur *et al.*, *Linac coherent light source (LCLS): Conceptual design report*, SLAC-R-593, UC-414 (2002).

[25] T. Tanaka and T. Shintake, eds., *SCSS X-FEL Conceptual Design Report* (RIKEN Harima Institute/SPring-8, 2005).

[26] M. Altarelli *et al.*, ed., *The Technical Design Report of the European XFEL*, DESY 2006-097 (2006).

[27] A. M. Weiner, Rev. Sci. Instrum. **71**, 1929 (2000).